

Detection of Sizes and Locations Air Voids in Reinforced Concrete Slab using Ground Penetrating Radar and Impact-Echo Methods

Nurhayati Abdul Razak, Syahrul Fithry Senin, Roszilah Hamid*

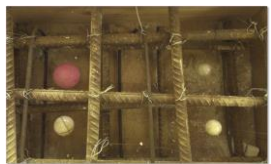
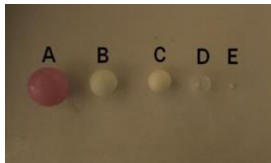
Department of Civil and Structural Engineering, Faculty of Engineering and Built Environment, Universiti Kebangsaan Malaysia, Malaysia

*Corresponding authors: roszilah@eng.ukm.my

Article history

Received : 7 January 2015
Received in revised form :
7 March 2015
Accepted : 8 April 2015

Graphical abstract



Abstract

The presence of inevitable air void defects in reinforced concrete components due to poor quality control during construction can further aggravate the moisture and chloride penetration in concrete to accelerate the corrosion process of the reinforcing steel. Non-destructive test (NDT) methods, Ground Penetrating Radar (GPR) and Impact-Echo (IE), are utilised to detect the void defects. This study is to compare the accuracy and limitations of both methods in detecting the sizes and depths of the air voids. The sample is a $600 \times 400 \times 200 \text{ mm}^3$ reinforced grade 40 concrete slab with embedded air voids in the sample. The air-voids are introduced in the concrete slab by positioning air-void plastic balls with diameters of 67, 45, 27, 20 and 3 mm each at the depths of 70, 80, 100, 80 and 80 mm, respectively, from the top surface of the slab. Results show that GPR can detect the air voids with sizes larger than 20 mm in diameter with error ranging from -8.9 to 30% from their actual diameters. The IE method is only able to detect the air voids depths and not the voids' sizes. It is also observed that the void depth estimation acquired by GPR is more accurate only for large size void (67 mm), but for sizes less than that, IE is more accurate in determining their locations. Both methods should be considered for NDT application in detecting voids depending on which parameter accuracy is anticipated.

Keywords: Air voids; reinforced concrete slab; ground penetrating radar; impact echo

Abstrak

Kewujudan kecacatan lompong udara di dalam komponen konkrit bertetulang akibat kawalan mutu yang rendah semasa pembinaan ditambah lagi dengan kehadiran lembapan dan penusukan klorida akhirnya boleh memecutkan proses pengkaratan tetulang. Radar Penusukan Bumi (RPB) dan kaedah Gema Hentaman (GH) digunakan untuk menentukan saiz dan kedalaman kecacatan lompong udara ini dalam papak konkrit bertetulang. Papak konkrit gred 40 bertetulang tersebut bersaiz $600 \times 400 \times 200 \text{ mm}^3$ dan lompong udara diwujudkan di dalam papak dengan meletakkan beberapa bebola plastik berlompong udara dengan diameter 67, 45, 27, 20 dan 3 mm pada kedalaman 70, 80, 100, 80 dan 80 mm daripada permukaan atas papak. Keputusan menunjukkan RPB boleh mengesan kewujudan lompong udara yang berdiameter lebih daripada dan sama dengan 3 mm dengan julat ralat di antara -8.9% sehingga 30 % daripada diameter sebenar. Kaedah GH pula didapati boleh mengesan kedalaman lompong udara tetapi tidak boleh mengesan diameter lompong udara. Keputusan kajian juga mendapati bahawa kedalaman lompong udara boleh dianggar dengan lebih jitu menggunakan RPB berbanding kaedah GH jika hanya saiz lompong adalah besar (67 mm), tetapi bagi lompong bersaiz lebih kecil dari tu, GH lebih tepat dalam menentukan kedudukannya. Kedua-dua kaedah perlu dipertimbangkan dalam mengesan lompong udara bergantung kepada parameter mana yang diperlukan ketepatannya.

Kata kunci: Lompong udara; papak konkrit bertetulang; radar penusukan bumi; gema hentaman

© 2015 Penerbit UTM Press. All rights reserved.

1.0 INTRODUCTION

Reinforced concrete is widely used in bridge construction in Malaysia¹. The bridge deck is the most important structural component that is necessary to safely transfer the heavy traffic loads to the other members. The safety of a deck is important to be preserved and maintained within its lifespan in order to ensure

its excellent performance to the users. However, the presence of inevitable air void defects in concrete due to poor quality control have been proven to reduce the concrete's compression strength². Annual inspection of bridges through visual inspection could not detect the present of air voids. The present of air voids can further aggravate the moisture and chloride penetration in concrete to accelerate the corrosion process of the reinforcing

steel. Bridge deck needs to be inspected for areas where there are voids, thus, area where the reinforcing steel are susceptible to corrosion.

Inspection of bridge deck requires rapid method as closing of bridge will obstruct traffic. The presence of voids in concrete can be detected by various non-destructive tests (NDT) including ultrasonic pulse velocity (UPV), ground penetrating radar (GPR) and impact echo (IE) tests. UPV method is not feasible for large area inspection and indirect method of measuring UPV is not accurate.

GPR offers a rapid, non-destructive and non-invasive investigation method for large concrete areas such as the bridge deck³. The method is based on the electromagnetic wave reflection principle, where the emitted waves from the transmitter antenna is partly reflected by the air void when propagating through concrete-air or air-concrete layer that possess contrast dielectric values, to the receiver antenna. The time taken between the emission and arrival of waves are recorded by the receiver antenna and stored in the GPR storage unit. Numerous efforts on using GPR to detect voids in concrete structures have been reported by various researchers and engineering practitioners. Gajda and Dowell⁴ have successfully located a number of voids located in Insulated Concrete Forms (ICF) structures. In another study at prestressed wall of box girder⁵, the researchers reported that none of the post-tensioning strands and simulated air voids within the grouted steel ducts was detectable, however, simulated voids within plastic ducts were generally detectable in GPR images. They concluded that the high dielectric constant of the steel ducts did not allow the microwaves to transmit through the surface of the duct and reach the simulated voids. Thus, they inferred that the void orientation is critical for detection in GPR images⁵. It can be concluded that the location of the void can be detected by GPR with limitation, but they did not mention that they had detected the sizes of the voids. The detection of small voids created in the concrete and voids developed during the concrete pouring operation also has been successfully studied⁶. They had detected gaps that developed between the foam and the concrete, voids intentionally created in the concrete, and voids that developed during the pouring operation but reported that small voids (e.g., less than $\frac{3}{4}$ in = 20 mm) were difficult to detect.

IE is another method that had made its way in non-destructive testing of concrete structure. The advantages of IE method is the test can be done on one surface, unlike UPV that requires both surfaces accessible. Voids detection in concrete using IE involves exciting concrete surface with a small mechanical impactor and measuring the reflected wave energy with a displacement transducer. A study was conducted to locate and to detect the presence of voids, however, they found that it becomes harder to detect the void as the bar spacing becomes narrower⁷. IE also had been concluded as a means of detecting voiding within plastic tendons⁸. A more recent study was conducted by a team of researchers using contactless IE method to detect the simulated voids in the grout fill within ducts and they able to determine the void detection probability in the duct⁹.

Based on the literature review, it is known that GPR and IE method can be used to identify and detect the voids in concrete. However, the range of void sizes and depth detected by both methods are not apparent in the many literatures. This paper is to study the detection of various sizes and depth of the artificial air void by both methods and comparing both methods effectiveness in assessing sizes and locations of voids.

2.0 METHODOLOGY

2.1 Materials

In this study, a concrete slab of 600 x 400 x 200 mm³ is cast in accordance with DOE Method¹⁰. Five artificial air voids as shown in Figure 1 are embedded at different depths and as shown in Figure 2 and Figure 3. Table 1 specifies the embedded depth of the artificial air voids inside the formwork before the concrete mixture of grade 40 is poured.

After the curing process for 28 days, the embedded voids in the sample were detected by GPR and IE method.

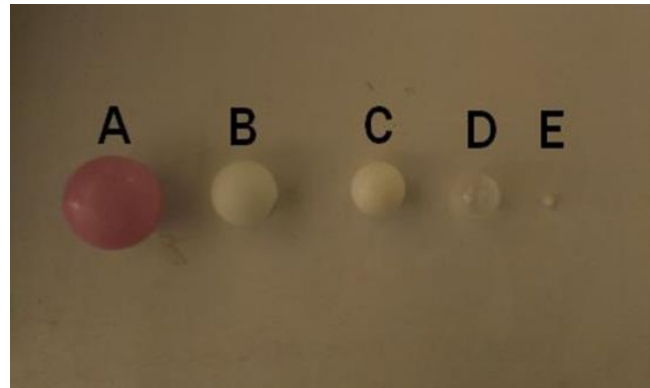


Figure 1 Artificial embedded air voids

2.2 GPR

GPR is used to detect the location of the air void and its sizes using the transmitter and receiver antenna. The current GPR antenna frequency used in this study is 1.6 GHz. The recorded data are then processed by Radan 7.0 to identify the voids' depths and their locations. The depth of the artificial air void is determined by subtracting the depth of the void-concrete and concrete-void locations in the radargram.

Table 1 Artificial air void sizes

Air Void	Sizes (mm)	Depth (mm)
A	67	70
B	45	80
C	27	100
D	20	80
E	3	80

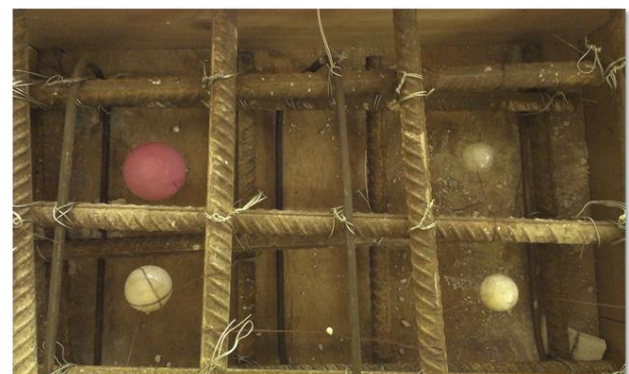


Figure 2 Location of artificial air voids in the slab

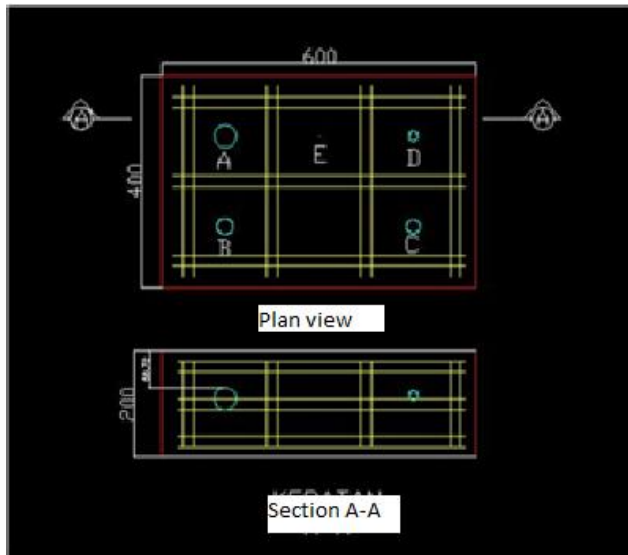


Figure 3 The configuration of artificial air voids in the sample (all dimensions are in mm)

2.3 IE

When the top surface of the slab was impacted by the steel ball, the wave propagates in the concrete and when it reach the surface of the voids and the bottom surface of the slab, the wave is reflected back to the top of the surface and is picked up by the transducer. The data is then recorded and analysed by Pi Scanner software. The analysis is given as a power spectrum plot in the form of amplitude signal versus frequency. The depths of the voids, *d*, are then estimated using Equation (1)¹¹.

$$D = 0.96 \frac{C_p}{2f} \tag{1}$$

where

D = void depth measured from the top surface (m)

C_p = concrete pressure (P) wave velocity (m/s)

f = frequency (Hz) of P-waves thickness mode

3.0 RESULTS AND DISCUSSION

3.1 GPR Data Interpretation

Figure 4 shows a typical recorded radargram by GPR on a grid that has been plotted on the slab surface directly above air void “A” placed in the slab after being processed by Radan 7.0. The electromagnetic wave reflection of the embedded void is represented as a bright layer when the GPR is scanned horizontally along the created slab grid for air void “A” embedded at 70 mm from top surface as shown in Figure 3. The distance from the top of the bright layer is denoted by *D*₂ and the bottom of the same layer is denoted by *D*₁.

Table 2 presents the sizes of the detected voids by subtracting the the depth of bottom layer of the void-concrete, *D*₁, from the top layer of concrete-void, *D*₂. It is observed that GPR can detect the air-void size that's larger than 3 mm in diameter with error ranging from -8.9 to 30 percent from its actual diameter. This analysis showed that the detected void sizes by GPR were slightly different to the original size of the voids. This might due to the squeezing of the plastic balls by the weight of the

concrete mix which reduce the original balls geometry. Void D is 0.020 mm in size and relatively small compared to the size of the other voids which contribute the highest error of detection of 30%. GPR can detect the sizes of voids but as the diameter of the voids reduced, the error in estimating the sizes increased.

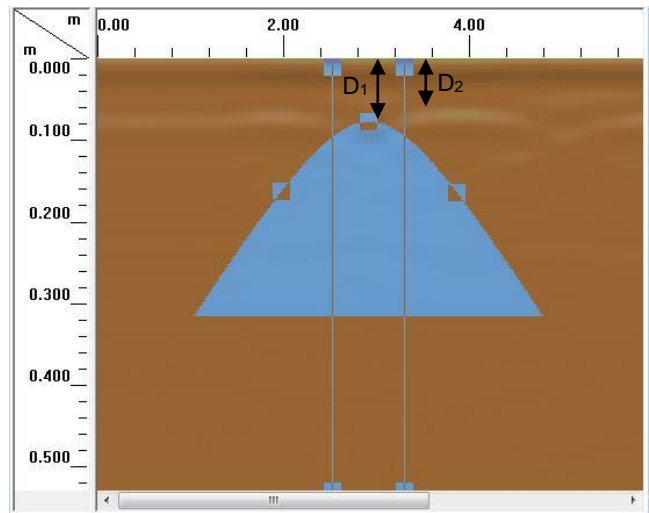


Figure 4 GPR radargram of air void for air void "A"

Table 2 Measured void sizes by GPR and its percentage error

Voids	Depth, <i>D</i> ₁ (m)	Depth, <i>D</i> ₂ (m)	Void size (<i>D</i> ₁ - <i>D</i> ₂) (mm)	% of error of original size
A	0.703	0.642	61	-8.96
B	0.890	0.867	43	4.44
C	0.779	0.748	31	12.90
D	0.861	0.835	26	30.00
E	ND	ND	ND	ND

ND – Not detected

3.2 Impact-Echo Interpretation

Figure 5 shows the typical power spectrum of IE signal of air void “A” embedded at 70 mm from the top slab surface. When the IE signal is reflected by the artificial air void, peak frequency is observed and the depth of air void can be estimated by Equation 1. Table 3 shows the peak frequency for the rest of the air voids and the estimated depths of air voids calculated using Equation 1.

From the data shown in Table 3, the higher frequency provides the deepest void of 0.880 m. Depth obtained by the impact echo test is also slightly different than the original depth of the void embedded in the slab. In addition, the depth of void E is not detected because its size is too small. For both data obtained from the GPR and IE tests, GPR had shown the capability of determining the size of the voids. The IE test can only determine the depth of the voids.

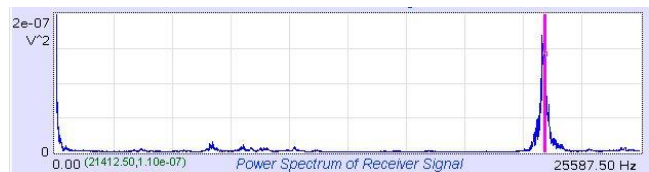


Figure 5 Power spectrum IE signal of air void "A"

Table 3 Computed void depths using Impact-Echo method

Void	f (Hz)	Computed depth (m)
A	21412.5	0.080
B	21275.0	0.083
C	21600.0	0.088
D	21150.0	0.080
E	ND	ND

ND – Not detected

3.3 Comparison between GPR and IE

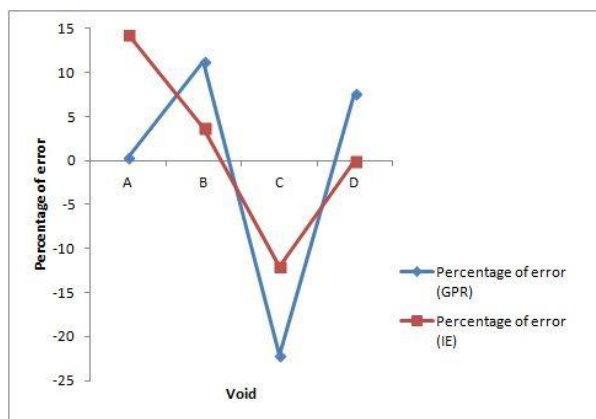
Comparison between the original depth of the void, the depth obtained from the GPR and the IE test is shown in Table 4. The percentage of error of actual depth is computed in Figure 6 using the Equation (2).

$$\text{Percentage of error} = \frac{(\text{Measured depth} - \text{Actual Depth})}{\text{Actual Depth}} \times 100 \quad (2)$$

Figure 6 shows that for large size void (67 mm), GPR is more accurate than IE in determining their locations but for smaller sizes voids (45 – 20 mm), IE estimates the voids location more accurately than GPR. This result may be attributed to the ununiform presence of moisture content in the slab that attenuates the GPR signals in a conductive environment as moisture content has significant effect on GPR signal.

Table 4 Differences of actual depth with GPR and IE estimation

Void	Actual depth (mm)	GPR (mm)	IE (mm)
A	70	70.3	80
B	80	89.0	83
C	100	77.9	88
D	80	86.1	80
E	80	-	-

**Figure 6** Comparison of percentage of error between GPR and IE in estimating depth of void

3.4 Comparison of the Minimum GPR Void Size Detection with Theory and Other Research

The performance of the current minimum void size detected by GPR is evaluated by comparing it with theoretical value and other

researcher's work¹². Theoretically, the minimum void size, D_{min} , that can be resolved by GPR can be estimated using Equation (3);

$$D_{min} = \frac{c}{4f\sqrt{\epsilon}} \quad (3)$$

where

- c = the speed of light in media vacuum
- f = the frequency of GPR antenna
- ϵ = the dielectric constant of the concrete

For the comparison purposes, the antenna frequency used by the present work must be almost similar to the other researcher work¹². The current GPR antenna frequency used in this study is 1.6 GHz. In this study, the dielectric values are taken as 9 as the concrete is cured, but not dry enough to take a lower value of dielectric constant⁶. Table 5 presents the theoretical minimum void size value, D_{min} , that also utilised 1.6 GHz antenna GPR frequency which has been used in this study.

Table 5 Theoretical D_{min} for 1.6 GHz GPR antenna frequency

D_{min} (mm)	Researcher
15.6	Theoretical (Eq. 3)
20	Current study
27	[12]

In this study, the experimental minimum detectable void size is 20 mm. However, a larger value of D_{min} was obtained from another researcher's work¹². The large value of the D_{min} value could be due to the attenuation and the clutter of GPR signals due to rebar, steel ties and plastic anchors embedded in the sample. In the present study, the void size characterisation is only limited clutter of GPR data caused by the rebar and the artificial air voids.

4.0 CONCLUSIONS

The size of the voids in the concrete sample can be detected by the GPR with errors ranging from -8.9 to 30% of their actual diameter. Impact echo test is, however, able to detect the location of the embedded voids in the sample, but cannot detect the size of the voids. Further consideration needs to be done before deciding on employing these NDT methods in detecting avoid in concrete structure depending on the intended outcomes.

Acknowledgement

The authors acknowledge financial support from Universiti Kebangsaan Malaysia through grants GUP-2013-017 and DLP-2013-033.

References

- [1] N. S. King and K. M. Mahamud 2009. *Bridge Problems In Malaysia*. Seminar in Bridge Maintenance and Rehabilitation, Kuala Lumpur.
- [2] P. Chindaprasit, S. Hanataka, N. Mistima, Y. Yuasa and T. Chareerat. 2009. Effects of Binder Strength and Aggrigate Size on the Compressive Strength and Void Ratio of Porous Concrete. *International Journal of Minerals, Metallurgy and Materials*. 16(2): 714–719.
- [3] A. H. A.Ghani, S. F. Senin and R. Hamid 2013. Attenuation of Ground Penetrating Radar Signals Amplitude in Monitoring Reinforced Steel Corrosion. *Jurnal Teknologi*. 65(2): 73–78.
- [4] J. Gajda and A. M. Dowell 2003. Concrete Consolidation and the Potential for Voids in ICF Walls. RD134. Skokie (IL): Portland Cement Association. 19.

- [5] D. G. Pollock, K. J. Dupuis, B. Lacour, K. R. Olsen 2008. Detection of Voids in Prestressed Concrete Bridges Using Thermal Imaging and Ground Penetrating Radar. Research Report, Washington State Transportation Center. 75.
- [6] C. Amer-Yahia and T. Majidzadeh 2012. Inspection of Insulated Concrete Form walls Using Ground Penetrating Radar. *Construction and Building Materials*. 26: 448–458.
- [7] T. Watanabe, T. Morita, C. Hashimoto and M. Ohtsu 2004. Detecting Voids in Reinforced Concrete Slab by SIBIE. *Construction and Building Materials*. 18: 225–231.
- [8] R. Muldoon, A. Chalker, M. C. Forde, M. Ohtsu and F. Kunisue. 2007. Identifying Voids in Plastic Ducts in Post-tensioning Prestressed Concrete Members by Resonant Frequency of Impact-echo, SIBIE And Tomography. *Construction and Building Materials*. 21: 527–537.
- [9] F. Schnefs, O. Abraham and J. S. Popovics 2012. Qualitative Evaluation of Contactless Impact Echo for Non-destructive Assessment of Void Detection Within Tendon Ducts. *Construction and Building Materials*. 37: 885–892.
- [10] Department of Environment. 1988. *Design of Normal Concrete Mixes*. Building Research Establishment, Watford, UK.
- [11] D. Sagar, R. Hamid and A. R. Khalim. 2011. Algorithm for Automatic Data Interpretation Software for Concrete Slab in Impact Echo Method. *Materials and Structures*. 45(5): 727–746.
- [12] R. Roger, C. Ken, A. Michael and S. Alan 2011. Insulated Concrete Form Void Detection Using Ground Penetrating Radar. PIERS Proceedings, Marrakesh, Morocco, March 20-23 2011. 1808–1815.